Reduction Kinetics of Fe_2MoO_4 Fine Powder by Hydrogen in a Fluidized Bed

R. MORALES, DU SICHEN, and S. SEETHARAMAN

Iron molybdate (Fe_2MoO_4) powders with an average particle size of 100 μm were reduced by hydrogen using a fluidized-bed batch reactor in the temperature range of 923 to 1173 K. The extent of the reaction was followed as a function of time by gas chromatography. The fluidizing-gas velocity was set at about 1.5 times the minimum fluidization velocity. The ratio of the height of the static bed to its diameter is about 1. Under the prevailing experimental conditions, it was found that the chemical reaction was the rate-controlling factor. The activation energy for this process was 158 $\pm$ 17 kJ/mol. The crystal size of the Fe_2Mo powder produced at lower temperatures was in the nanometer range, indicating the possibility of mass production of alloys and intermetallics in the nanorange, using a fluidized bed.

I. INTRODUCTION

THE increasing demand for different nanoscale materials for applications in advanced technology has led to the development of suitable methods for the bulk production of these nanomaterials. Earlier investigations[1,2] in the present laboratory have shown that the gas-solid reaction route offers an excellent potential for the production of nanostructured intermetallics. The two most important aspects identified in this respect are the initial particle size and processing temperature. A small initial precursor particle size and a low reaction temperature would favor the production of nanostructured powders, without the occurrence of sintering between the particles and grain growth. In this respect, a fluidized-bed process could be an attractive alternative, as it provides good gas-solid contact and helps to minimize temperature variations.

The experimental studies on fluidized systems have been mainly confined to the effect of operating variables of gas flow through granular solids. In a fluidized-bed reactor, the reaction rate may be controlled by any of the following reaction steps:

1. chemical reaction,
2. diffusion through the product layer,
3. mass transfer in the gas phase, or
4. a combination of these steps.

Very little has been done to study the possibility of using a fluidized bed to produce nanostructured intermetallics. The aim of the present investigation is twofold:

1. to evaluate the feasibility of producing nanostructured Fe_2Mo in a fluidized-bed reactor by the reduction of Fe_2MoO_4 using hydrogen and
2. to establish the reaction kinetics of the reduction of Fe_2MoO_4 in a fluidized bed.

R. MORALES, Scientist, is with the Instituto de Investigaciones Metalurgicas, UMSNH, Santiago Tapia 403, Morelia, Mich. 58000, Mexico. DU SICHEN and S. SEETHARAMAN, Professors, are with the Department of Materials Science and Engineering, Royal Institute of Technology, SE-100 44 Stockholm, Sweden. Contact e-mail: raman@kth.se

Manuscript submitted August 28, 2002.

II. EXPERIMENTAL

A. *Materials*

The iron molybdate powder used in this work was synthesized using iron, Fe_2O_3, and MoO_3. The specifications of these materials are listed in Table I. The starting materials were mixed in stoichiometric proportions and compacted into pellets. These pellets were placed in an iron crucible, and the crucible was sealed hermetically by welding an iron lid on its top. The crucible containing the sample was heated to 923 K and kept at this temperature for 24 hours. Thereafter, the sample was heated to 1473 K and kept there for another 24 hours to allow sintering. The crucible was then quenched in water. The composition and microstructure of the Fe_2MoO_4 prepared by this method were examined by X-ray diffraction (XRD) using a PHILIPS* x-pert system and by scanning electron microscopy (SEM) using a JEOL* model JSM-840. Figure 1 shows the nature of Fe_2MoO_4 particles at different magnifications. It can be seen that the particles consist of a matrix of small crystals. The XRD analysis revealed a highly crystalline specimen with the diffraction-line position corresponding to Fe_2MoO_4 phase, as shown in Figure 2. The particle-size distribution was obtained by dynamic light scattering using a Coulter LS 100 Q apparatus (Coulter International Corp., Miami, FL). The average particle diameter (d_p) was found to be 100 μm, as shown in Figure 3. Hydrogen was used as the reactant gas for the fluidized-bed reduction, while argon was employed during the heating and cooling modes. Both gases were plus grade (maximum 10 ppm impurities) and were supplied by AGA Gas (Stockholm).

*PHILIPS is a trademark of Philips Electronic Instruments Corp., Mahwah, NJ.

*JEOL is a trademark of Japan Electron Optics Ltd., Tokyo.

B. *Apparatus*

Figure 4 shows a schematic diagram of the fluidized-bed reactor used in the experiment. The reaction column consists of a quartz tube, 15-mm i.d. and 1-m long. The gas distributor

Table I. Specification of the Materials Used in the Synthesis of Fe_2MoO_4

Compound	Purity (Pct)	Supplier
Fe_2O_3	99.8	Alfa Aesar (Karlsruhe, Germany)
MoO_3	99.95	Alfa Aesar
Fe	98	Merck (Darmstadt, Germany)

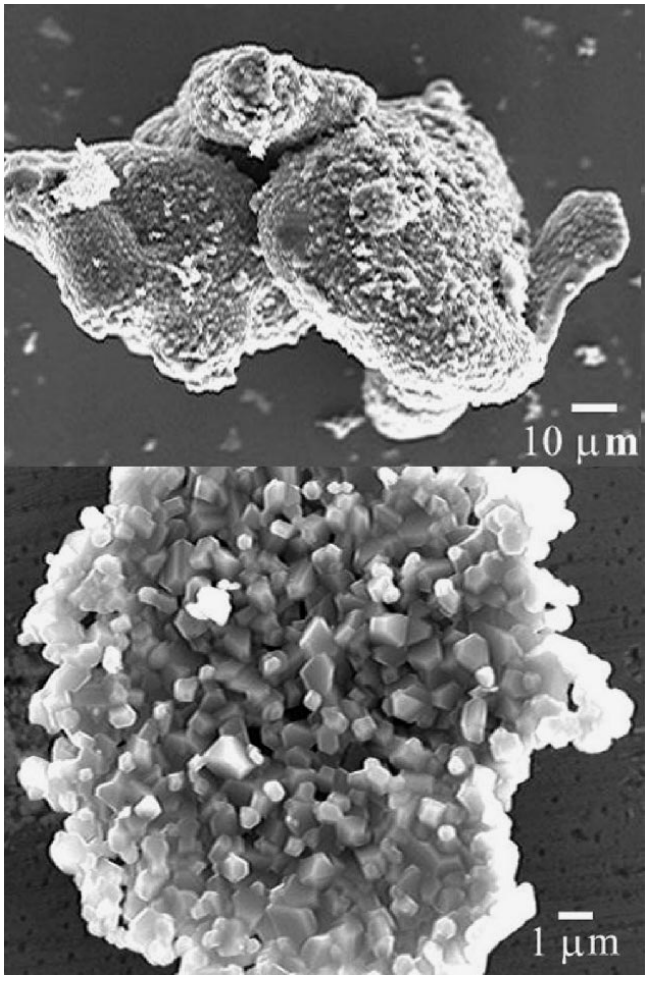

Fig. 1—SEM pictures showing the nature of the initial fluidizing particles.

was a 2-mm-thick porous quartz plate (average pore size of 200 μm). A rotameter was used to control each of the flow rates of hydrogen and argon before entering the reactor tube through the bottom. The off-gases were conducted through a stainless steel tube of 5-mm i.d. The end of the tube was coupled to a "T" joint followed by stainless steel ball valves, in order to direct the gas stream adequately. The majority of the off-gas was led to a Shimadzu gas chromatograph, model GC-9AM, with a TCD detector (Shimadzu Corp., Kyoto, Japan). Hydrogen was employed as the carrier gas in the gas chromatograph. The whole stainless steel line, including the valves, was wrapped up with heating tape to prevent any condensation of H_2O before it reached the gas chromatograph.

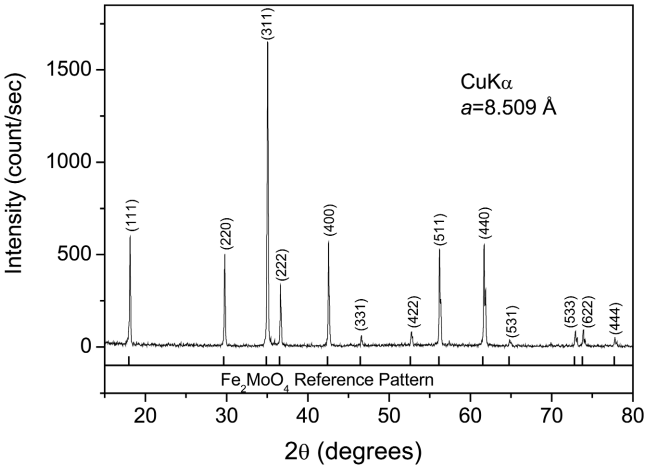

Fig. 2—XRD pattern of the initial fluidizing powder revealing Fe_2MoO_4 phase.

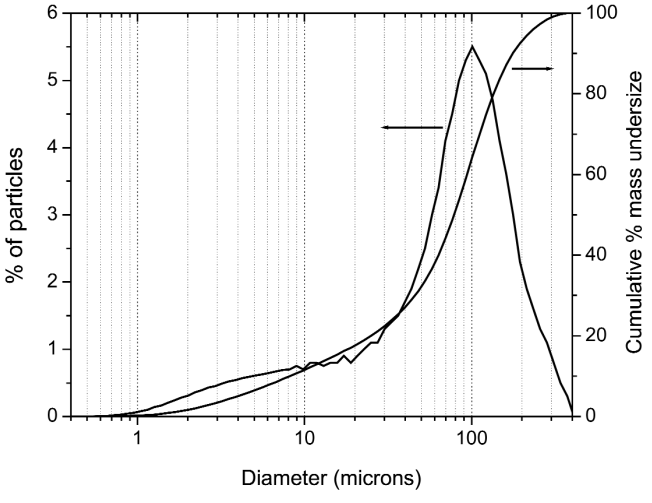

Fig. 3—Particle size distribution analysis of Fe_2MoO_4.

C. *Procedure*

To ensure a good fluidization, the minimum fluidization velocity (U_{mf}) was determined experimentally by pressure-drop measurements at room temperature. In order to determine the net pressure drop in the powder bed, the total pressure drops in the reactor with and without the powder bed were measured independently. The net pressure drop was then taken as the difference between the two pressure drops. The fluidization velocity at a higher temperature was then evaluated from the values at room temperature (U^*_{mf}), by taking into account the decrease in density and increase in viscosity of hydrogen due to temperature increase,[3] namely,

$$U_{mf} = U^*_{mf} \frac{\rho_r \mu_r}{\rho_T \mu_T} \qquad [1]$$

where ρ_r and μ_r and ρ_T and μ_T are the density and viscosity of the fluidized gas at room temperature and at higher temperature, respectively.

The U_{mf} value obtained experimentally at room temperature was found to be about 2.3 cm/s, which corresponded to a flow rate of 0.16 L/min, as shown in Figure 5. The estimated U_{mf} and the fluidizing-gas velocity (U_f) at different working temperatures are shown in Table II. It was decided to operate close to the minimum fluidization velocity to avoid (or at least minimize) the elutriation of the finest particles, as well as the formation of bubbles in the emulsion. According to Hovmand *et al.*,[4] laboratory-sized reactors are particularly prone to slug-flow regime when $(U_f - U_{mf}) > 1.0$ cm/s with a height-to-diameter ratio of $H/D > 1$. For the present experimental conditions, $(U_f - U_{mf}) < 1.5$ cm/s with H/D of about 1, the breakdown of fluidization by slug-flow behavior is not likely to occur. Therefore, a well-mixed solid suspension is expected to occur under these conditions of gas-fluidization velocity and H/D ratio.

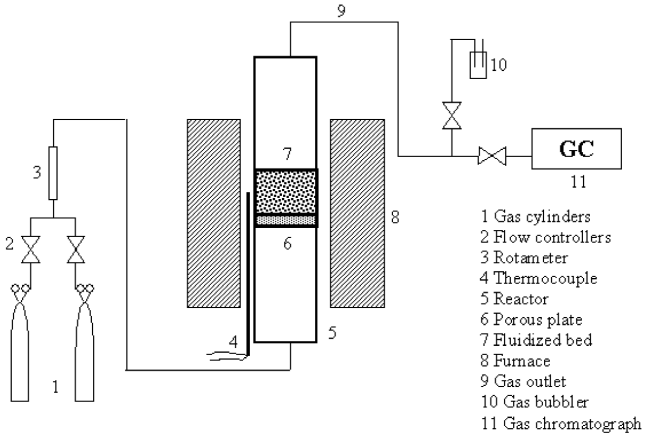

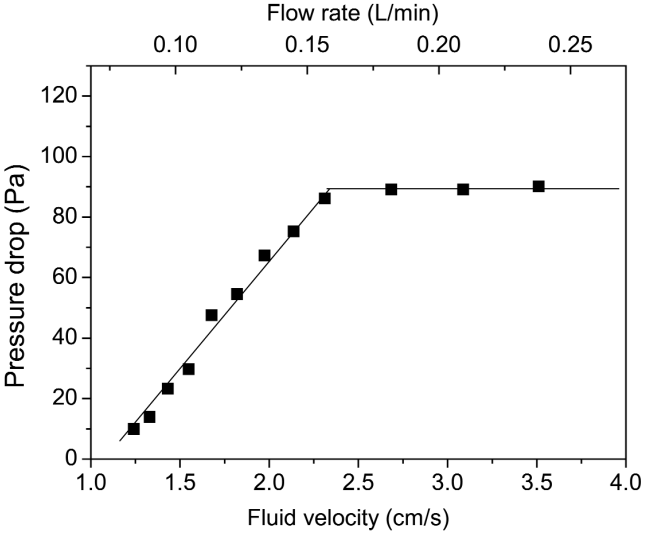

Table II. Summary of Fluidization Conditions

d_p (μ)	T (K)	U_{mf}* (cm/s)	U_{mf}** (cm/s)	U_f** (cm/s)	U_f** (mL/min)
100	294	2.3	—	—	—
—	923	—	2.47	3.76	258
—	973	—	2.54	3.85	265
—	1023	—	2.59	3.94	271
—	1073	—	2.65	4.03	276
—	1123	—	2.70	4.11	282
—	1173	—	2.75	4.19	287

*Measured at room temperature.
**Estimated values at different working temperatures.

The fluidized-bed reduction experiments were conducted isothermally. Typically, a charge weight of 2 g was used, which gave a static bed with an H/D ratio of about 1. This charge was placed in the constant-temperature zone of the furnace. A type-S thermocouple was placed in direct contact with the exterior of the fluidized-bed reactor near the porous quartz plate. The reactor was heated electrically using a temperature-controlled vertical tube furnace (Eurotherm-94, Arlöv, Sweden). During the heating stage, argon was passed through the reactor. When the temperature of the reactor was stabilized at the predetermined value, the argon gas was replaced by hydrogen. The water phase in the off-gases produced by the reaction of iron molybdate with hydrogen was quantitatively monitored by gas chromatography. When no more traces of water in the system were detected, the hydrogen gas was replaced by argon, indicating the end of the reduction. It should be noted that the time taken for the product gas to reach the gas chromatograph after the onset of the reaction was about 25 seconds. This elapsed time was determined using preliminary experiments.

The reduced fraction was estimated in the following manner. During the reduction process, the relative concentration of water in the system was shown in the gas chromatograph in the form of peaks. The area of these peaks (A_P) was plotted as a function of time. On the basis of this plot, the integration of $A_P(t)dt$ was normalized to 100 pct reduction and the reduced fraction was, thus, calculated backwards. The value of the integration of the curve was found to be consistent at every reduction temperature.

III. RESULTS

The reduction curves obtained from the fluidized-bed reactor are shown in Figure 6. The degree of reaction is described as a reduced fraction, defined as the ratio of the weight change (ΔW) to the theoretical final weight change (ΔW_∞):

$$X = \frac{\Delta W}{\Delta W_\infty} \qquad [2]$$

The value of X can also be described by the ratio of the area under the curve $A_P(t)$ against *time* at an instant t to the area at the time the reaction ends, namely,

$$X = \frac{\int_0^t A_p(t)dt}{\int_0^\infty A_p(t)dt} \qquad [3]$$

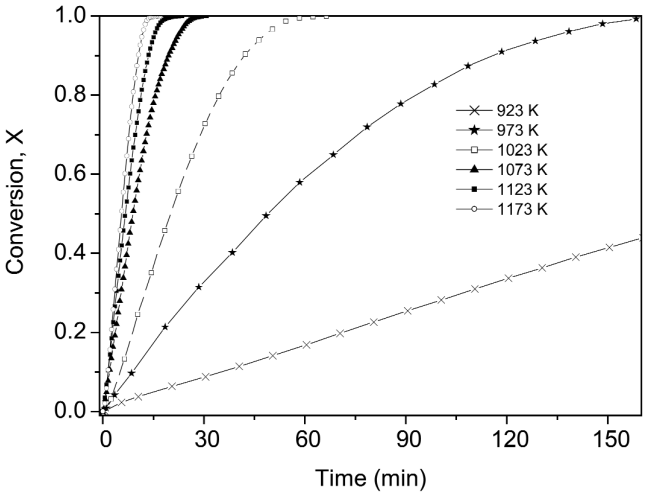

Fig. 6—Experimental results of the fractional reduction against time at various temperatures.

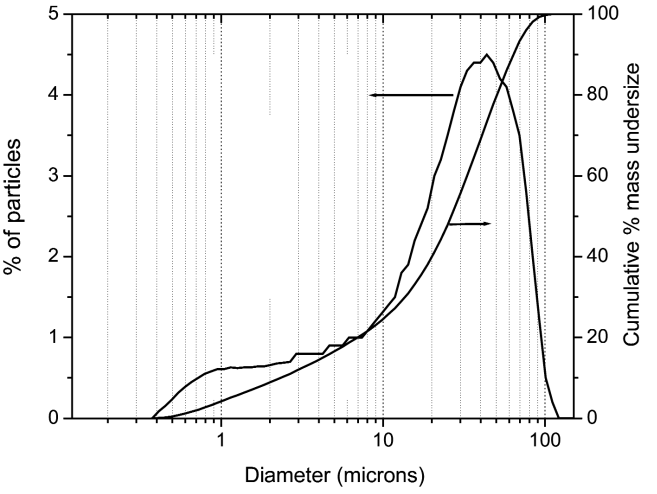

Fig. 8—Particle size distribution analysis of Fe_2Mo.

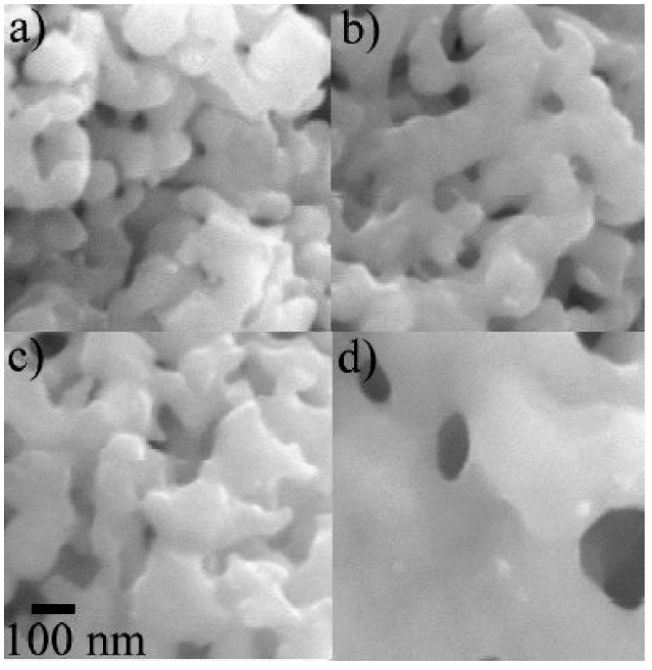

Fig. 7—SEM micrographs showing the effect of reduction temperature on the microstructure of fine fluidizing powder: (*a*) 923 K, (*b*) 1023 K, (*c*) 1073 K, and (*d*) 1173 K (all at the same magnification).

From Figure 6, it can be seen that reduction rate increases dramatically with the increase of temperature. While it takes only about 10 minutes for the complete reduction at 1173 K, the reaction was extremely slow at 923 K. In fact, after 9 hours of processing, the reduced fraction was estimated to be only 0.91.

Earlier studies of kinetics[1] and characterization[2] have shown that the reduction of Fe_2MoO_4 by hydrogen occurs in one step according to the following reaction:

$$0.25Fe_2MoO_4 + H_2 = 0.25Fe_2Mo + H_2O \qquad [4]$$

Micrographs of the reaction product revealed that the reduction process transformed a solid reactant particle into a multiple-product-particle agglomerate. In order to examine the effect of temperature on the morphology of the reduced sample, scanning electron microscope (SEM) analysis was carried out. Figures 7(a) through (d) present the SEM micrographs of the samples reduced at 923, 1023, 1073, and 1173 K, respectively. It can be seen that small particles are interconnected by "necks," forming a porous network. The coalescence of the necks at 1173 K is dramatic in comparison with the reduction products at lower temperatures. It is interesting to note that the reduction at 973 K would result in a fine crystal size in the micron region. The average particle size of the end powder processed at 973 K was measured and was found to be 30 μm, as shown in Figure 8. It should be mentioned that the elutriation of the finest particles was not noticeable in the experiments, and no elutriation procedure was taken. The SEM micrographs in Figures 7(a) through (d) represent the common structures of the reduced samples.

IV. DISCUSSION

It is seen in Figures 7(a) through (d) that a lower reduction temperature would favor the production of metallic powders with nanoscale crystals. As shown in Figure 7(a), the crystals are well below 100 nm. On the other hand, the crystal size is much bigger at 1173 K. In order to ascertain the production of nanomaterials through the fluidized-bed reduction route, the mechanism of the reduction should be examined.

The reduction of Fe_2MoO_4 by hydrogen in a fluidized bed consists of a number of steps, namely,

1. mass transfer in the gas phase,
2. gas diffusion through the product layer,
3. chemical reaction at the interface between the unreacted core and the product layer, and
4. the heat transfer from the reaction zone to the surroundings, caused by the enthalpy change of the reaction.

A. *External Mass Transfer as a Possible Rate-Controlling Step*

It is well known that the resistance of the gas film decreases as the particle size decreases, resulting in a higher value of the mass-transfer coefficient (h_m).

Since mass transfer through the gas film is a physical phenomenon, its sensitivity to temperature can be considered to be small. An estimation of h_m at 1073 K could be indicative of the resistance of the gas film in the present experiments. The convective mass-transfer coefficient is related to the Sherwood number by the following relationship:

$$\mathrm{Sh} = \frac{h_m L}{D_{AB}} \qquad [5]$$

Where D_{AB} is the interdiffusion coefficient of species A in a gas mixture of A-B, and L is the characteristic length, namely, the particle size, in the present case. For a particle in a flowing gas stream, the Sherwood number could be calculated using the following empirical expression:

$$\mathrm{Sh} = 2.0 + 0.6\,\mathrm{Re}^{1/2}\,\mathrm{Sc}^{1/3} \qquad [6]$$

In the present work, the interdiffusion coefficient of water vapor and hydrogen was estimated at 1073 K using the equation by Slattery and Bird.[5] The D_{AB} value was evaluated to be 25.48 cm^2/s. Although the use of the equation by Slattery and Bird has been reported to be less satisfactory[6] for the H_2O-H_2 mixture, this equation can still predict the order of magnitude of the interdiffusion coefficient of the system with sufficient accuracy for the present discussion. On the basis of the present experimental conditions and the evaluated D_{AB} value, the value of h_m at 1073 K is estimated using Eqs. [5] and [6], taking an average particle size of 100 μm (Figure 3). The calculation yields a value of 5165 cm/s for h_m. This extremely high value indicates that external mass transfer is less likely to be the rate-controlling step.

B. *Diffusion of H_2 and H_2O through the Product Layer as the Possible Rate-Controlling Step*

When diffusion through the product layer controls the rate of reaction, the experimental data of the reduced fraction (X) against *time* should follow the following expression, if a shrinking-core model can be applied:[7]

$$1 + 2(1 - X) - 3(1 - X)^{2/3} = \frac{6M_s b D_{AB,eff}(C_{Bo} - C_{Bc})t}{\rho_s r_o^{\,2}} \qquad [7]$$

Where r_o is the initial particle radius, b is the stoichiometric coefficient, $D_{AB,\,\mathrm{eff}}$ is the effective diffusion coefficient, ρ_s and M_s are the density and molecular weight of Fe_2MoO_4, respectively, and C_{Bo} and C_{Bc} are the gaseous reactant molar concentration at the external and unreacted core interfaces, respectively. With no external mass-transfer resistance, $C_{Bo} \approx C_{B\infty}$, and the concentration difference in Eq. [7] is assumed to be constant. In this case, the left-hand side of Eq. [7] will be a linear function of time.

It should be pointed out that Eq. [7] is valid for powder assemblies having a uniform particle size. On the other hand, as shown in Figure 3, the particles used in the experiments had not very wide size distribution. Hence, Eq. [7] could still be employed semiquantitatively to examine the possibility of diffusion control. The right-hand side of Eq. [7] at 1073 K is plotted as a function of time in Figure 9. The substantial deviation of the plot from a linear relationship indicates that the diffusion through the product layer is unlikely to be the controlling step.

C. *Chemical Reaction as the Rate-Controlling Step*

It is seen in Figure 6 that the reaction rate strongly depends on temperature. This strong dependence would suggest a chemical-reaction controlling mechanism. From the discussion so far, the gas diffusion through the product layer and external mass transport as rate-controlling steps are not likely to be rate controlling. In view of the fluidization and very small particle size, heat transfer could also be assumed to be less important for the overall kinetics. This strengthens the case for a serious consideration of the chemical reaction as the rate-determining step.

The rate constants at different temperatures can be obtained from the experimental data using the "shrinking"-core model. If Reaction [4] is of first order with respect to hydrogen and is irreversible, the relationship between the reaction time t and the reduced fraction X for chemical-reaction control is expressed as [7]

$$1 - (1 - X)^{1/3} = \left(\frac{b \cdot M_s \cdot k \cdot C_{Bg}}{\rho_s \cdot r_o}\right) \cdot t \qquad [8]$$

where k is the rate constant and C_{Bg} represents the concentration of hydrogen in the gas stream. Assuming that ρ_s, r_o, M_s, k, and C_{Bg} remain constant at a given temperature, Eq. [8] can be rewritten as

$$1 - (1 - X)^{1/3} = \left(\frac{k_r}{r_o}\right) \cdot t \qquad [9]$$

where k_r is a new constant. The term $(1 - (1 - X)^{1/3})$ should be a linear function of time if the reduction is controlled by the chemical reaction at the interface between the product

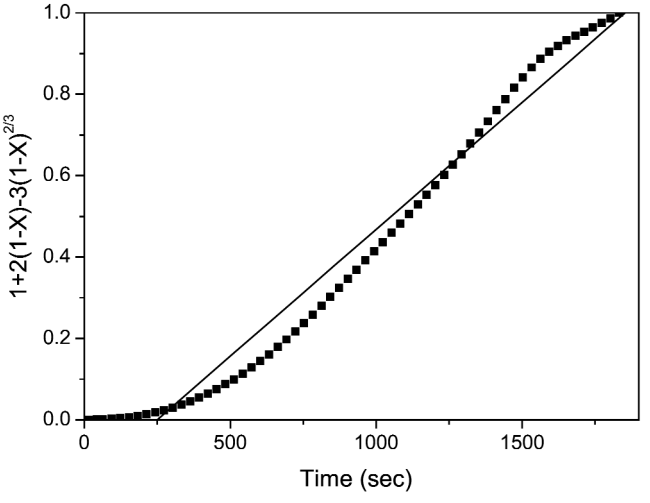

Fig. 9—Experimental values and theoretical linear fit corresponding to the product layer resistance for the reduction of Fe_2MoO_4 by hydrogen at 1073 K.

layer and the unreacted core in each particle. To encounter the particles with a range of size distributions, Filippou *et al.*[8] have suggested an elegant way of processing the experimental data. The powder bed can be assumed to contain particles of a number of small size ranges. The size range (i) can be assumed to have an average initial radius of $r_{0,i}$. The overall reduced fraction can be described as

$$X = \sum_i w_i X_i \qquad [10]$$

where w_i and X_i stand, respectively, for the mass fraction and reduced fraction of particles having an initial radius of $r_{o,i}$. The value of w_i can be evaluated from Figure 3 for the size range i, while X_i can be described by Eq. [9].

The value of k_r at each temperature was evaluated by a nonlinear least-squares method. On the basis of the experimental data at a given temperature, a value of k_r was sought that minimized the error sum (S):

$$S = \sum_j (X_j - <X_j>)^2 \qquad [11]$$

In Eq. [11], X_j is the experimentally determined reduced fraction at time t_j and $<X_j>$ is the overall reduced fraction estimated using Eqs. [9] and [10]. Five size ranges were taken to evaluate k_r. The size fractions employed, along with the size ranges and the evaluated values of w_i, are presented in Table III. The estimated values of k_r by least-squares fittings are listed in Table IV. The correlation coefficients are also listed in this table. It is seen that the values of R^2 are very close to 1, which is in conformity with the chemical controlling mechanism.

The temperature dependency of the rate constant k_r of Reaction [4] can be determined by an Arrhenius plot, namely, ln k_r *vs* 1/T.

$$k_r = k_o \exp\left(-\frac{Q}{RT}\right) \qquad [12]$$

Table III. Fe_2MoO_4 Particle Size Fractions Used for the Estimation of k_r by Least-Square Fittings

i	$r_{i\ \min}$ (μm)	$r_{i\ \max}$ (μm)	$r_{0,i} = (r_{i\ \min} * r_{i\ \max})^{1/2}$ (μm)	w_i
1	0.57	11.36	2.55	0.018
2	11.36	28.88	18.11	0.072
3	28.88	50.55	38.21	0.23
4	50.55	88.45	66.86	0.39
5	88.45	186.5	128.43	0.29

Table IV. Estimated Values of k_r by Least-Squares Fittings

T (K)	k_r(μm/s)	R^2
923	7.4×10^{-4}	0.9731
973	2.75×10^{-3}	0.9844
1023	6.22×10^{-3}	0.9914
1073	1.36×10^{-2}	0.9818
1123	1.85×10^{-2}	0.9844
1173	2.14×10^{-2}	0.9847

Where k_o is a constant, Q stands for the activation energy for the reaction, T is the temperature in Kelvin, and R is the gas constant. The k_r values listed in Table IV are plotted against 1/T in Figure 10. As it can be observed, the experimental values corresponding to the temperatures 1123 and 1173 K lie somewhat below the regression line. This could be attributed to the sintering effect, which would reduce the area of the reaction surface and, thus, decrease the reaction rate to some extent. In fact, slight sintering of particles was observed when the samples were taken out from the reactor at temperatures above 1073 K. Hence, the points corresponding to 1123 and 1173 K were left out in the calculation of the activation energy. The value of the activation energy for the Reaction [4] obtained from the slope of the plot in Figure 10 was 158 ± 17 kJ/mol. This high value suggests again that the chemical reaction is most likely the rate-controlling step for temperatures below 1123 K.

In an earlier work, Morales *et al.*[1] studied the hydrogen reduction of Fe_2MoO_4 in thin powder beds using a higher flow rate of hydrogen as well as smaller particle size; they obtained an activation energy of 173 kJ/mol for the reduction of Fe_2MoO_4 by hydrogen gas. This value is close to the activation energy calculated in the present study, 158 ± 17 kJ/mol.

The formation of Fe_2Mo intermetallic phase has been controversial. While some investigators were unable to detect this phase during diffusion-couple experiments[9,10] or during annealing of compact powders,[11,12,13] some research groups have detected the Fe_2Mo phase by aging Fe-Mo alloys.[14–17] Sinha *et al.*[18] reviewed the controversial evidence concerning the formation of Fe_2Mo and came to the conclusion that the rate of formation of the phase is very slow. The present result clearly shows that production of Fe_2Mo particles is possible by gas-solid reduction in a fluidized-bed reactor. The reduction of Fe_2MoO_4 renders a uniform distribution of highly reactive Fe and Mo particles as nearest neighbors and results in a single-step reaction. These particles are then likely to react with each other by means of surface reaction and grain-boundary

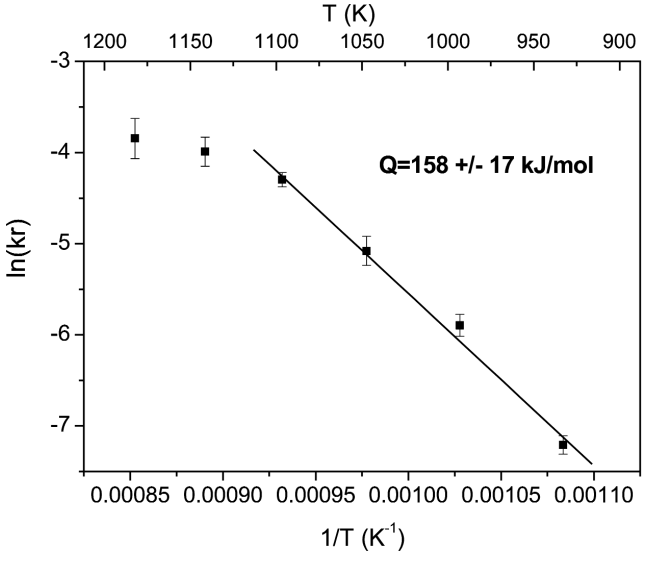

Fig. 10—Arrhenius plot for the reduction of Fe_2MoO_4 by hydrogen.

diffusion, leading to uniform composition. This mechanism is favored by the fluidization conditions. Thus, the gas-solid reaction route with fluidization appears to be a very promising route toward the production of the Fe_2Mo phase with a nanocrystalline structure.

The present results provide important information for the design of a large-scale reactor to produce nanostructured Fe_2Mo. The use of fine particles with an average particle size of 100 μm in a fluidized-bed reactor leads to a process with a chemical-reaction rate-controlling step. Increasing the particle size will gradually increase the contribution of both external mass transfer and diffusion in the product layer. The reduction process at lower temperatures results in a nanostructured product of Fe_2Mo, as shown in Figure 7. The crystal size of the product increases with the increase of temperature. On the other hand, a lower temperature results in a very low reaction rate. In order to achieve this microstructure, both the crystal size of the product as well as the reaction time are to be optimized. The present experimental results suggest that a reaction temperature as low as 973 K would be preferable. Also, a fluidizing-gas velocity just above the minimum fluidization velocity was found to be more than adequate in achieving the aforementioned results. The use of a low flow rate would favor to the optimum consumption of hydrogen.

V. CONCLUSIONS

In this work, fine powder of Fe_2MoO_4 was reduced with hydrogen gas using a fluidized-bed reactor. It was found that, by using a fluidizing-gas velocity 1.5 times higher than the minimum fluidization velocity, for an average particle size of 100 μm and an H/D ratio of about 1, the reduction process was controlled by the rate of the chemical reaction of the particle. The activation energy for this process was found to be 158 ± 17 kJ/mol. The kinetic data obtained in this work can be of use for designing a large-scale reactor for the bulk production of nanoscale-sized particles of Fe_2Mo and other similar intermetallic materials.

ACKNOWLEDGMENTS

The authors are thankful to The National Council for Science and Technology (CONACYT, Mexico) for supporting one of the authors, R. Morales, during his stay in Sweden.

REFERENCES

1. R. Morales, I. Arvanitidis, Du Sichen, and S. Seetharaman: *Metall. Mater. Trans. B*, 2002, vol. 33B, pp. 589-94.
2. R. Morales, V. Agarwala, and S. Seetharaman: *J. Mater. Res*., 2002, vol. 17 (8), pp. 1954-59.
3. M.A. Doheim, M.Z. Abdel-Wahab, and S.A. Rassoul: *Metall. Trans. B*, 1976, vol. 7B, pp. 477-83.
4. S. Hovmand, W. Freedman, and J.F. Davinson: *Trans. Inst. Chem. Eng*., 1979, vol. 49, pp. 149-62.
5. J.C. Slattery and R.B. Bird: *AIChE J*., 1958, vol. 4, pp. 137-42.
6. J. Zsekely, J.W. Evans, and Y.H. Sohn: *Gas-Solid Reactions*, Academic Press, New York, NY, 1976, p. 18.
7. O. Levenspiel: *Chemical Reaction Engineering*, John Wiley & Sons, New York, NY, 1962, ch. 12.
8. D. Filippou, N. Katiforis, N. Papassiopi, and K. Adam: *J. Chem. Technol. Biotechnol*., 1999, vol. 74, pp. 322-28.
9. R.D. Rawlings and C.W.A. Newey: *J. Iron Steel Inst*., 1968, vol. 206, p. 723.
10. C.P. Heijwegen and G.D. Rieck: *J. Less-Common Met*., 1974, vol. 37, pp. 115-21.
11. S.R. Baen and P. Duwez: *J. Met*., 1951, vol. 3, pp. 331-35.
12. J.W. Putman, R.D. Potter, and N.J. Grant: *Trans. ASM*, 1951, vol. 43, pp. 824-47.
13. H. Kleykamp and V. Schauer: *J. Less-Common Met*., 1981, vol. 81, pp. 229-38.
14. R.P. Zaletaeva, N.F. Lashko, M.D. Nesterova, and S.A. Yuganova: *Dokl. Akad. Nauk. SSSR*, 1951, vol. 81, pp. 415-16.
15. C.J. Bechtoldt and H.C. Vacher: *J. Res. NBS*, 1957, vol. 58, pp. 7-19.
16. J. Higgings and P. Wilkes: *Phil. Mag*., 1972, vol. 25, pp. 599-623.
17. T. Miyazaki, S. Takagishi, H. Mori, and T. Kozakai: *Acta Metall*., 1980, vol. 28, pp. 1143-53.
18. K. Sinha, R.A. Buckley, and W. Hume-Rothery: *J. Iron Steel Inst*., 1967, vol. 205, pp. 191-95.